

UNDERSTANDING AND SUPPRESSING FIELD EMISSION USING DC

E. MAHNER

*Fachbereich Physik, Bergische Universität Wuppertal,
Gaußstraße 20, D-42097 Wuppertal, Germany*

(Received 8 March 1994; in final form 28 March 1994)

In this review, dc studies of the enhanced electron emission from broad area polycrystalline niobium cathodes of high purity are presented. On a microscopic scale the characterization of individually localized sites was carried out by the use of a purpose built UHV field emission scanning microscope and a scanning electron microscope including an energy dispersive x-ray detection. These tools were used to investigate the effects of heat treatment cycles between 200°C and 1400°C on the field emission properties of Nb cathodes. Broad area surfaces of cm² size which do not emit at 100 MV/m were repeatedly obtained after heat treatments at T = 1400°C. New emitter appeared if such emission-free cathodes were annealed again at 600°C–800°C. In addition, the results of a series of measurements are reported in which various kinds of particles with known geometry and composition were intentionally placed on niobium and gold substrates. It seemed that the interface between this kind of field emitter and the substrates did not play an important role in the mechanism of enhanced electron emission. In several experiments on high purity niobium samples of the same material the dependence of the electron field emission behaviour on incremental material removal was studied. These samples had been prepared by the use of a high pressure ultrapure water rinsing technique. No systematic dependence between emitter density and material removal between 4 μm and 84 μm was observed at a surface field of 100 MV/m. But, in contrast to earlier investigations the electron emission always originated from material irregularities without the presence of microscopic particles sticking on the surface.

KEY WORD: Superconducting RF

1 INTRODUCTION

It is well known that on macroscopic metal cathodes subjected to high electrical fields in vacuum electron field emission is observed.¹ The emission of prebreakdown currents starts in the macroscopic gap field range of 5–20 MV/m which is much below the value of 3 GV/m predicted by the Fowler-Nordheim law for flat, metallic surfaces. In early years the most favoured model assumed a metallic field emission at surface microprotrusions or whiskers.² At these sites the macroscopic gap field is geometrically enhanced by a factor β that results in a microscopic field exceeding the Fowler-Nordheim field emission law. As a consequence high voltage electrodes were mechanically polished to obtain a smooth and mirror-like finish. This procedure did not result in reliable suppression of enhanced field emission (EFE). With the use of modern electron microscopy it became apparent that in most

cases such whisker failed to be present on virgin electrodes.³ More recently two new types of *in situ* anode probe techniques for locating and studying individual emission sites were developed. In the first system a specimen is scanned in front of an anode probe hole and a field emitting site is localized by a current detector behind the hole.⁴ In the second technique the sample is scanned in front of a micropoint anode.^{5,6,7} It turned out that the scanning needle technique has the advantage of a higher spatial resolution by using sharp tips and small gap sizes. In addition high field investigations ($E > 100$ MV/m) are possible because only a small specimen area beneath the anode probe can be subjected to a high field. In consequence, the use of different anode geometries has the advantage to zoom from low to high resolution FE scans on broad area cathodes.⁸ In order to study the nature of EFE both systems were incorporated into UHV surface analysis systems containing Scanning Electron Microscopy (SEM), Auger Electron Spectroscopy (AES), and x-ray Photoelectron Spectroscopy (XPS or ESCA: Electron Spectroscopy for Chemical Analysis).^{6,9,10} These studies have shown that often particles of micrometer size or foreign material inclusions which show a big variety of elemental composition are responsible for enhanced field emission.¹⁰ Metallic protrusions are very rarely the cause of EFE. The spectral characteristics of the emitted electrons were recently studied with a high resolution spectrometer.¹¹ As a result the electrons are emitted from individual subsites having single peak spectra and a strong field dependence shift from the Fermi level of the cathode towards low energies.¹² These electron spectroscopy studies of the emission process indicated that the emission is non-metallic in origin. Latham and co-workers developed a field-induced hot electron emission model that proposes a metal-isolator-metal-vacuum (MIMV) microstructure which is responsible for EFE.^{13,14} A detailed description of the field-induced hot electron emission mechanism that should occur at conducting channels in MIM devices is given in the literature.¹ Measurements of electron emission images were performed with an energy selective display technique.¹⁵ The results have been qualitatively explained with a coherent scattering process of hot electrons at the edge of a metal-isolator-metal microstructure. In addition, a transparent anode imaging spectrometer including a scanning laser probe was developed to study the effects of laser induced transient surface heating on the electron emission of high voltage electrodes.¹⁶ The laser beam energy flux was varied and different conditioning mechanism were observed. This latter technique seems to be interesting for future small area and surface limited heating procedures that do not influence the bulk material.

2 EXPERIMENTAL

Full details of our experimental technique and measurement procedure that have been developed for the localization of field emitting sites on broad area cathodes are reported elsewhere.⁸ In short our experimental arrangement consists of a multi-function UHV surface analysis system ($3 \cdot 10^{-11}$ mbar) including a Scanning Electron Microscope (SEM). A purpose built high resolution field emission scanning microscope consists of an UHV micromanipulator that allows precise cathode motions along the x -, y - and z -axes. For specimen alignment a tilt facility is incorporated. At a rotatable holder seven anodes with different tip geometries for high and low resolution FE scans are mounted. With a fast high

voltage regulator used in a “threshold” or constant current mode a distribution of weak and strong field emitting sites is obtained by scanning the sample. During the FE scans the high voltage gap is controlled with a resolution of $2\ \mu\text{m}$ by means of an external long distance microscope and a CCD video camera. To precisely locate the coordinates of the emitting sites an automatically searching procedure is initiated in which the cathode is scanned in a raster pattern. After a microadjustment of the cathode position the gap size and the I-V characteristic are automatically measured and plotted. With these techniques we locate field emitter to an accuracy of $0.2\ \mu\text{m}$ and a reproducibility of $\leq 5\ \mu\text{m}$, respectively. The UHV system also contains a separately pumped preparation chamber ($1 \cdot 10^{-9}$ mbar), a fast entry airlock, and a sample transport system. Without removal from UHV samples can be heat treated up to 2000°C by electron bombardment. The heating unit was calibrated with an infrared pyrometer to a precision of 20°C and a minimum temperature of 200°C . In the preparation chamber a facility for dust free exposure of the cathode to pure gases is also installed.

At Saclay the scanning field emission apparatus is based on a commercial SEM equipped with an energy dispersive x-ray detection system (EDX) that allows to identify elements with atomic numbers down to six. The SEM chamber pressure is normally $\approx 1 \cdot 10^{-6}$ mbar. The microscope is modified for field emission measurements by the addition of a tungsten anode ($\varnothing \approx 80\ \mu\text{m}$) that can be retracted during the SEM and EDX examination of a sample. A regulated high voltage up to 6 kV is applied to the anode and any current flowing between the anode and cathode is detected with a picoamperemeter. A detailed description of the apparatus is given in the literature.¹⁷

3 SAMPLE PREPARATION

From high purity niobium 10 polycrystalline samples were machined into 16 mm diameter flat disks of 2 and 3 mm thickness. In order to avoid electrostatic edge effects all cathodes had rounded top edges. The disks were put onto special niobium holders that fit to the sample transport system of our apparatus. To remove the surface damage layer 4 cathodes were chemically polished ($100\ \mu\text{m}$) at Wuppertal with a standard recipe (BCP 1:1:1) which is used for preparing high quality Nb RF cavities.¹⁸ A final rinsing in ultrapure water was always performed in our cleanroom. The samples are mounted under lamina flow in a special developed transport box that avoids a surface contamination with dust particles. The most important security facility consists of a cleaned stainless steel hat protecting the cathode surface. This cap is only removed in the preparation chamber under UHV. The other 6 niobium samples were prepared at CEBAF (USA) by a gradual removal of the surface damage layer between $4\ \mu\text{m}$ and $84\ \mu\text{m}$ using a 1:1:1 BCP. The most important difference to our preparation technique was a 20 min rinsing with ultrapure high pressure water (≈ 85 bar) and a final methanol rinsing. This water rinsing procedure has a high possibility to remove all particles sticking on the polycrystalline, rough cathode surface. For shipping the same sample transport system was used.

4 RESULTS ON NONE HEAT TREATED SURFACES

After sample alignment in the microscope all virgin cathodes were systematically scanned with a 1 mm and 0.5 mm diameter anode at $I \leq 10\text{--}20$ nA. The FE scans were performed between 40 MV/m and 100 MV/m with a gap of 170 μm . With this procedure we detect the distribution of strong and weak emitting sites on broad area cathodes in one single scan. The gap and I-V characteristic of each localized site are measured after centering the anode carefully above the maximum of emission. Fowler-Nordheim plots are always made with the 0.5 mm anode. In addition each field emitting site was individually scanned with a microtip anode at a reduced gap of 20–40 μm and SEM images were obtained.

On non heat treated samples prepared in Wuppertal 5–7 field emitter per cm^2 were found at 100 MV/m and $I \leq 10$ nA. All localized FE sites were associated with micron-sized particles, mechanical defects like microscratches or etch pits. It is remarkable that a big number of additional particles are present on the cathode which do not emit up to 100 MV/m. For one sample the density of particles (1–8 μm) was counted to $\approx 120/\text{cm}^2$, but only 8 particles/ cm^2 were active field emitter.

In Saclay various kinds of particles (≈ 20 μm) with known composition were intentionally placed on plane Nb and Au cathodes.¹⁷ On niobium substrates no emission up to 100 MV/m was found from insulating particles like Al_2O_3 and SiO_2 and particles with insulating oxide layers (Nb, Ti). In contrast, oxide free particles (Au, Ag) and those with a conducting oxide (Fe) were identified as strong FE sites. Similar results were obtained for gold substrates. The low threshold field of ≈ 40 MV/m for field emission from gold particles on a gold substrate was surprising. The interface between particle and substrate (mechanically polished with an alumina slurry) is expected by the authors to be metallic without the presence of an insulator. Experiments with Fe and Ag particles on anodized (240–270 nm) niobium showed that the presence or absence of the anodized oxide appears to make little difference. In addition, evidence of melting was found at the interface between Fe particles and the Nb substrate. These structures were found to emit strongly. In consequence, there is evidence at Saclay that strong field emission may occur from metallic particles due to the simple projection model without the insulating interface assumed by the antenna model. In a second experimental step measurements were performed to test the applicability of the projection model by the use of artificial FE sites. Nickel particles of varying geometry were placed on Nb and Au substrates.¹⁹ The irregular Ni particles (5–10 μm) were associated with “good” emitter while at 90% of spherical particles (10–20 μm) no emission was seen up to 120 MV/m. These experiments were repeated with iron particles with similar results, again no significant difference was seen between Nb and Au substrates. No relation between particle size (2–30 μm) and field emission threshold was found for irregular FE sites.

By the use of a diamond tool (commercial phonograph stylus) artificial “point” defects and “scratch” defects were produced on Nb and Au substrates. These kind of sites were observed to be strong sites that are more stable than the field emission from superficial particles. A possible chemical contamination on the scratch resulting from the stylus was excluded because no foreign elements were found in the EDX analysis. The method of site creation and their similar FE behaviour on Nb and Au substrates suggested the possibility of projections on the cathode surfaces. In order to overcome the problem to find projections of sufficient sharpness a “projection on a projection” model has been proposed that explains

both the observed geometry and the measured β of the artificial sites.¹⁹ Supported by numerical calculations an overall field enhancement factor $\beta = \beta_1 * \beta_2 = (h_1/r_1) * (h_2/r_2)$ of the order of 100 can be achieved with two superposed hemispherically capped structures with realistic microscopic dimensions, for example $h_1 = 10 \mu\text{m}$, $r_1 = 1 \mu\text{m}$, $h_2 = 100 \text{ nm}$, and $r_2 = 10 \text{ nm}$. Indeed, such geometrical protrusions were observed with the electron microscope on some artificial scratch defects at Saclay. In summary, the Saclay experiments seem to indicate that an oxide between intentionally positioned particles and the substrate (Nb and Au) does not play an important role. Artificial particles and scratches might behave as geometrical protrusions with an additional field enhancement at its apex.

For further interpretation one has to keep in mind that a poor vacuum will probably influence the Fowler-Nordheim characteristic of the FE sites as well as the interface between particle and substrate. In addition, EDX may not be sensitive enough to exclude that the contact between particle and substrate is completely free of a thin insulating area. Nevertheless, superficial metallic particles and mechanical damage sites are potentially strong sources of electron emission.

5 HEAT TREATMENT

A heat treatment of high voltage cathodes is well known as an important conditioning effect for the influence of field emission. One important basic requirement is UHV ($\leq 10^{-9}$ mbar) in the analysis chamber in order to get reproducible results. Studies with copper²⁰ and niobium²¹ cathodes have shown that a rise in temperature can increase the total gap current through stimulating the switch on of new emission sites. On niobium surface heat treatments at 400°C–900°C increased the average emission strength of the emitter and their density, while at higher temperatures the number of sites decreased drastically.¹⁰ In previous studies we have already shown that a high temperature UHV annealing at $T \geq 1200^\circ\text{C}$ resulted in a high probability of destroying individual FE sites on Nb cathodes.⁸ In the following chapter we present studies in order to give an answer to the important (fundamental and technological) question: Does a “low temperature” heat treatment of emission free Nb surfaces stimulate the creation of new field emitting sites on high RRR bulk niobium?

In order to study a possible creation and evolution of FE sites one sample was selected that showed a representative emitter density after the first (as introduced) scans. The principal results of the first series of heat treatments between 1400°C and 200°C are shown in Figure 1. From the series of scans at 100 MV/m it is evident that the density of sites is strongly reduced after the high temperature treatment at 1400°C and 1200°C. Obviously there is a sharp increase in the number of sites (13) after 600°C. Further heat treatments at 400°C and 200°C switched off 5 sites while 6 field emitter were activated at these low temperatures. In consequence, the number of sites was almost unchanged between 600°C and 200°C but their distribution changed. A HT at 1400°C during the second thermal cycle (Figure 2) switched off all FE sites and an “electrically clean” surface was obtained at 100 MV/m. *In situ* SEM studies showed that 64% of the active sites after 200°C were unchanged, 14% disappeared, and 22% changed their appearance. During the second cycle we also observed an increase in the density of field emitting sites after firing at 800°C and 600°C. Heating at 400°C and 200°C switched on 13 additional sites. In consequence, we created a total number of 31

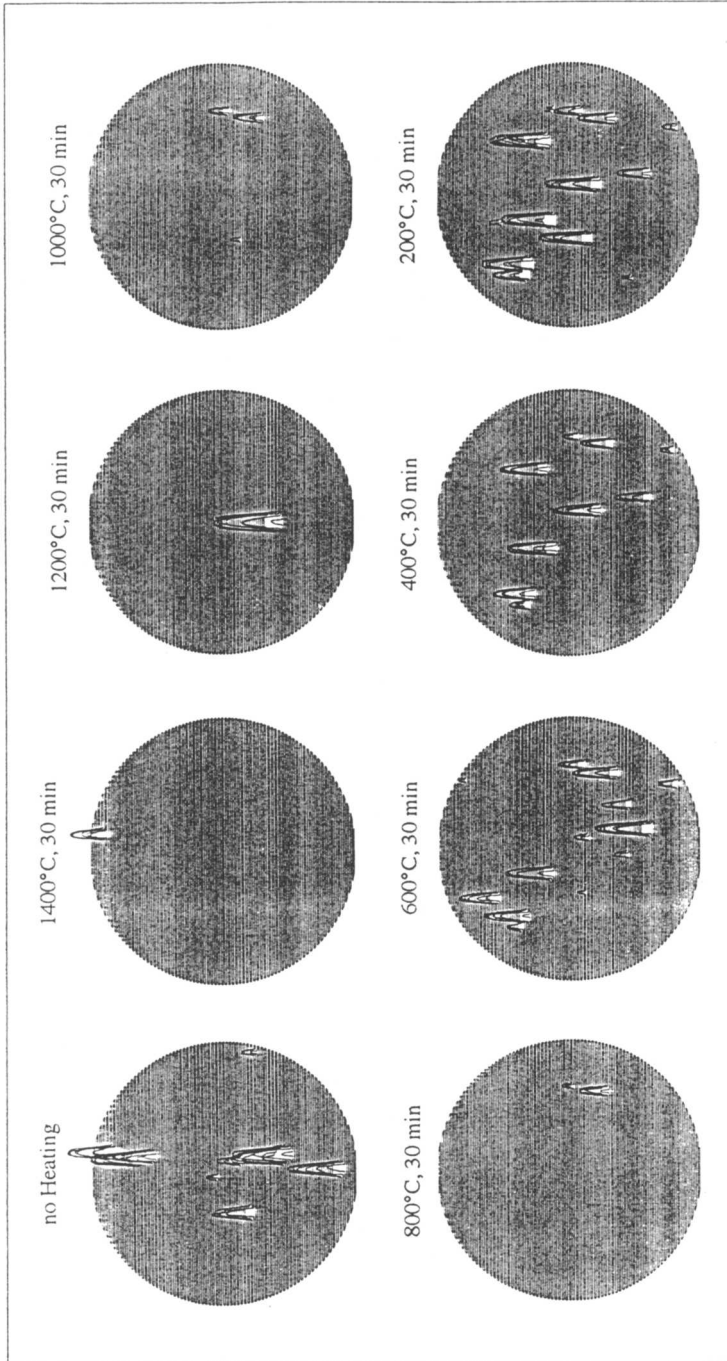


FIGURE 1: Selection of FE scans (\varnothing 15.0 mm) at 100 MV/m on high purity niobium as a function of HT (first thermal cycle). The scans were made with a \varnothing 0.5 mm anode and $I < 10$ nA.

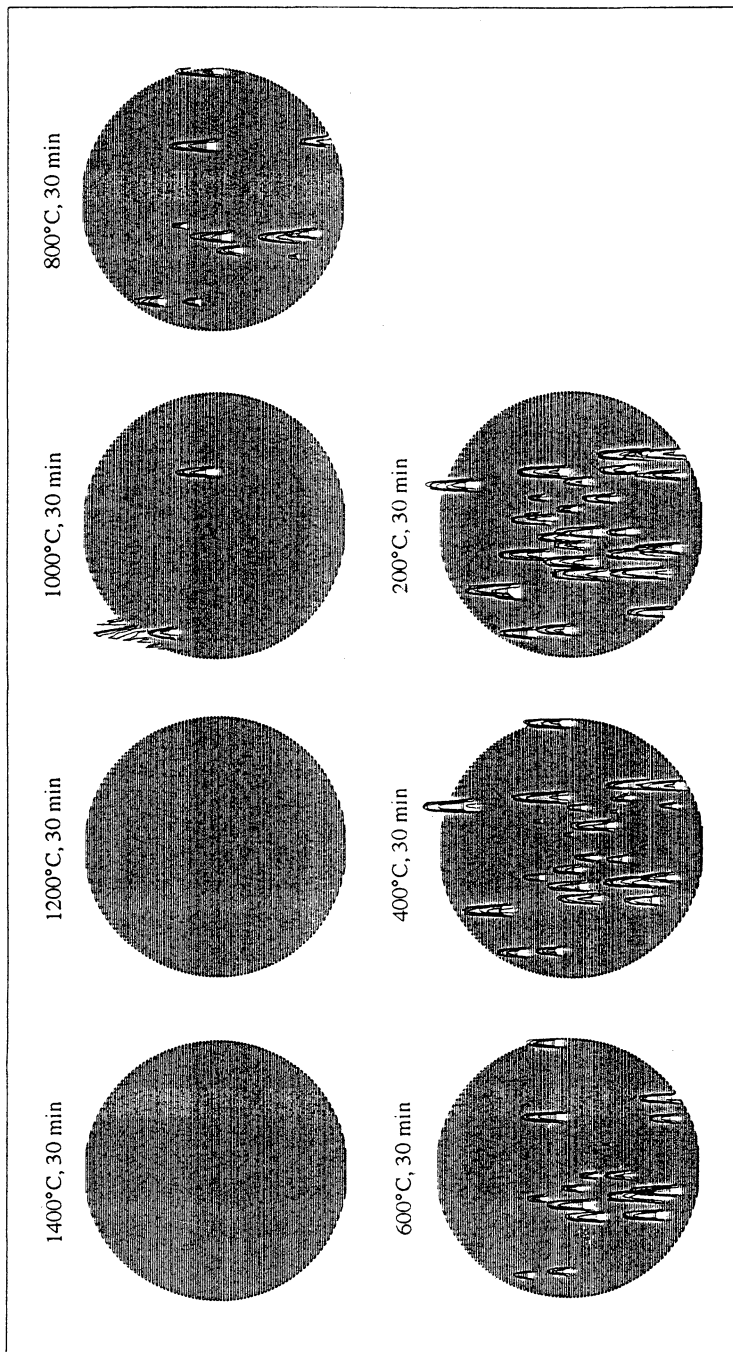


FIGURE 2: Selection of FE scans (\varnothing 15.0 mm) at 100 MV/m (same sample as in Figure 1) as a function of HT (second thermal cycle). The scans were made with a \varnothing 0.5 mm anode and $I < 10$ nA.

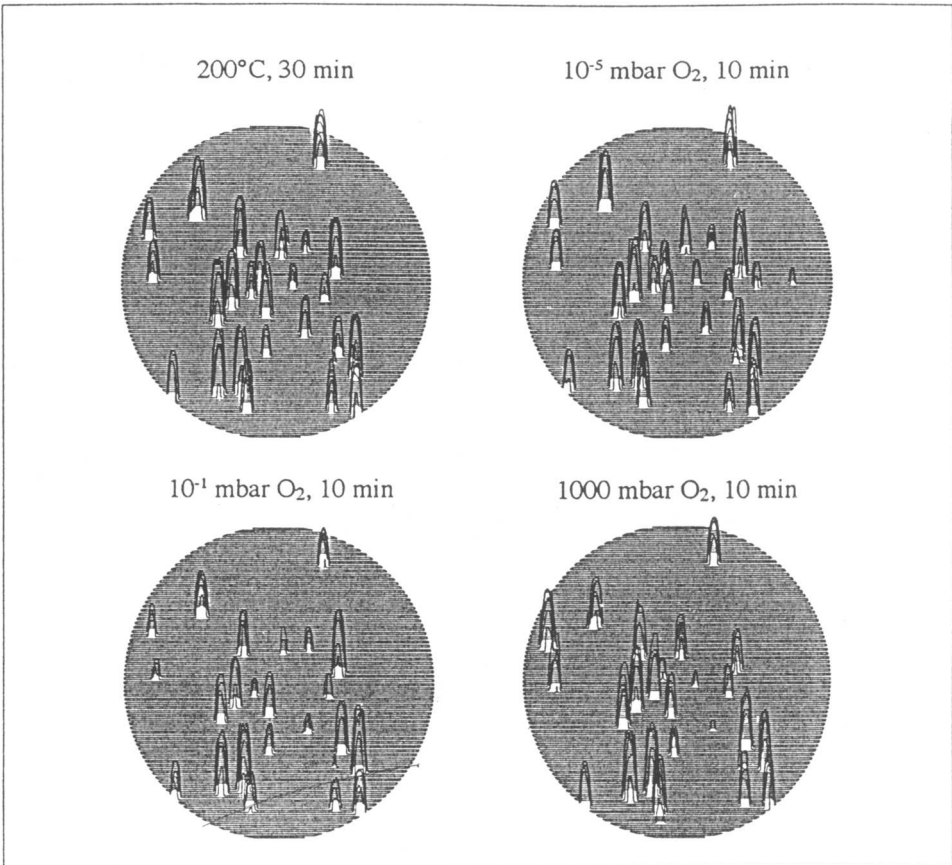


FIGURE 3: Subsequent field emission scans ($\varnothing 15.0$ mm) at 100 MV/m (on the same sample as in Figure 1 and Figure 2) after gas exposure with pure O_2 in the preparation chamber. The scans were made with a $\varnothing 0.5$ mm anode and a limiting current of 10 nA.

active sites by subsequent UHV heat treatments below 1200°C . It is remarkable that none of the localized emitter in the first thermal cycle was identified as a site in the second cycle.

In order to study the influence of absorbed O_2 on the field emission characteristics of the localized sites we carried out gas exposure experiments. The oxidation process was performed in the preparation chamber with pure O_2 . The cathode was subsequently exposed to 10^{-5} mbar, 10^{-1} mbar, and 10^{+3} mbar O_2 for always 10 min and scanned at 100 MV/m with the 0.5 mm diameter anode. Figure 3 shows that there is no influence on the density of FE sites and their spatial distribution after oxidation. On that sample a total number of 64 different sites was localized. In order to determine the individual characteristic of each site 210 gap measurements and 390 Fowler-Nordheim plots were carried out during the heat treatment and oxidation tests. The onset value for FE activity (E_{onset}) resulted from the slope of the gap measurement in the constant current mode (0.5 nA) of the microscope.

The values of β and S were derived from the FN plots. In summary, E_{onset} varied between 32 MV/m and 91 MV/m while β and S scattered from 7–150 and 10^{-8} – 10^{-16} cm². The evolution of E_{onset} , β and S was studied individually for all sites. It turned out that no general trend was observed in the two thermal cycles and the oxidation experiments. Most of the sites showed a stable FE behaviour changing their β and E_{onset} between 10% and 30% with no correlation to the heating temperature. Calculating an average value for β and E_{onset} for each site it is remarkable that most of the sites did not change their β and E_{onset} more than $\approx 20\%$. No correlation was found between the physical size of the emitter and the S values from the Fowler-Nordheim fit. If the emission mechanism is more complex than a simple projection model this is not surprising because the size of the “active electron source” remains unclear even with the use of a high resolution SEM.

6 SURFACE ANALYSIS

After the heat treatment and oxidation experiments the sample was carefully transferred to an UHV surface analysis system ($2 \cdot 10^{-10}$ mbar) containing a SEM, microfocus Auger, and scanning Auger of $0.2 \mu\text{m}$ resolution with a CMA analyzer.²² In addition, an argon ion gun was used for sputtering and depth profiling. The entire sample surface contained a thin contamination layer (≤ 1 nm) of C and O due to adsorption. The oxid layer was determined to be less than 12 nm. After emitter localization point Auger spectra were taken on 14 active FE sites. In addition a background measurement at a distance of $\approx 5 \mu\text{m}$ from the emitter was always performed as a reference. It was found that the analyzed sites contained Al, W, Ca, Ti, Cu, S, C, O, Nb. A typical example is given in Figure 4. At the reference points (Nb, C, O) generally no foreign elements were detected in the Auger spectra. After sputtering C and O disappeared in the reference and only Nb was detected. In 50% of the sites an enhanced concentration of C or O was found. After sputtering (4 sites) additional impurities of Ti, Si, Cs, C, and O were found “inside” the particles. In two cases non field emitting micron-sized particles were detected. At these spots the Auger spectra were identical with the impurity free reference data. The emitter displayed in Figure 5 looked like a “mole-hill” with a size of $\approx 6 \mu\text{m}$. This site contained only Cu and S with small amounts of C. Scanning Auger mapping measurements $80 \mu\text{m} \cdot 80 \mu\text{m}$ around the emitter showed that Cu and S were sharply located at the site position and did not spread around the “particle”. In order to determine the emitter composition point Auger spectra were taken after gradually sputtering to ≈ 30 nm (Figure 6). Only small additional Nb peaks occurred to the peaks observed on the surface indicating that no other contaminations are present.

7 DISCUSSION

The increase in the density of field emitting sites was reproducibly observed on high purity bulk niobium in the temperature range of 600°C – 800°C . Even emission free surfaces at 100 MV/m were activated after a low temperature heat treatment resulting in an emitter density of $\approx 18/\text{cm}^2$. Mostly isolated particles with random shape were found in the SEM.

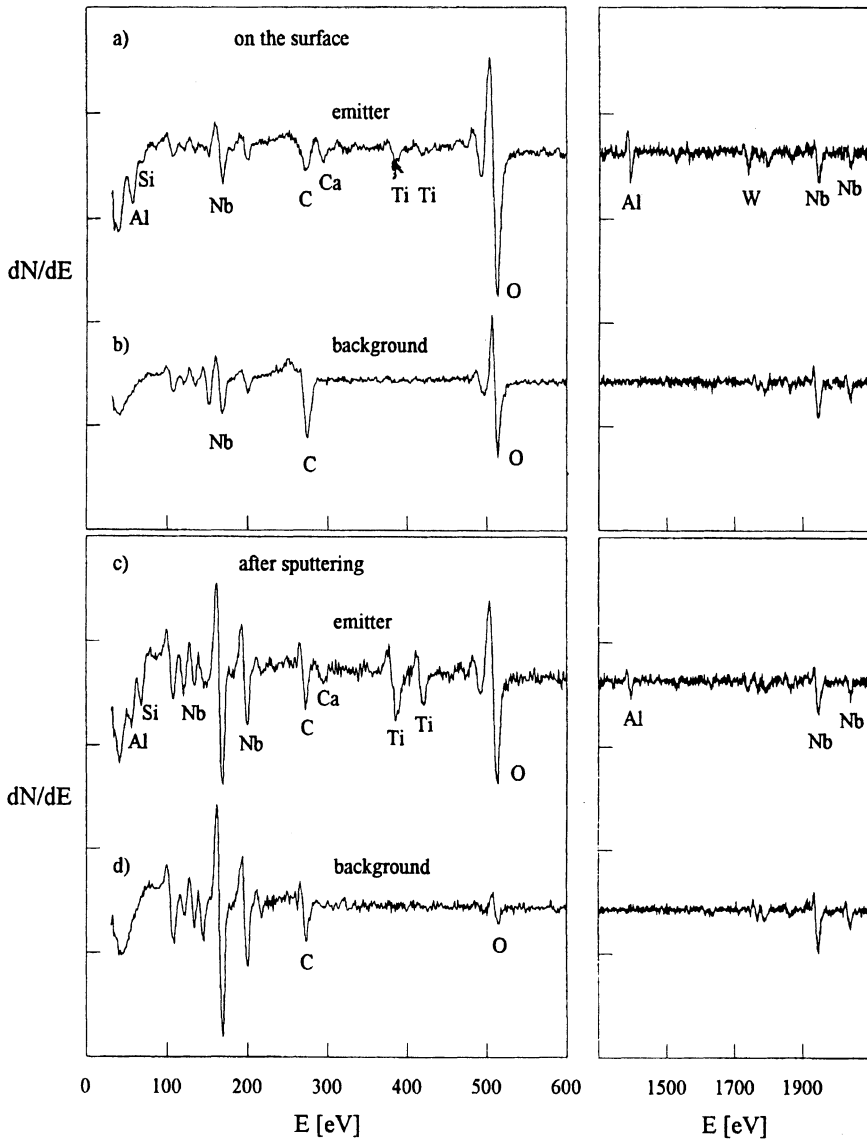


FIGURE 4: Auger spectrum of an emitting particle containing Al, Si, Nb, C, Ca, Ti, O, and W. (a) Point Auger spectrum on the FE site, (b) Auger spectrum of the nearby ($\approx 5 \mu\text{m}$) background Nb surface. (c)–(d): same as (a) and (b) after sputter removal of $\approx 60 \text{ \AA}$.

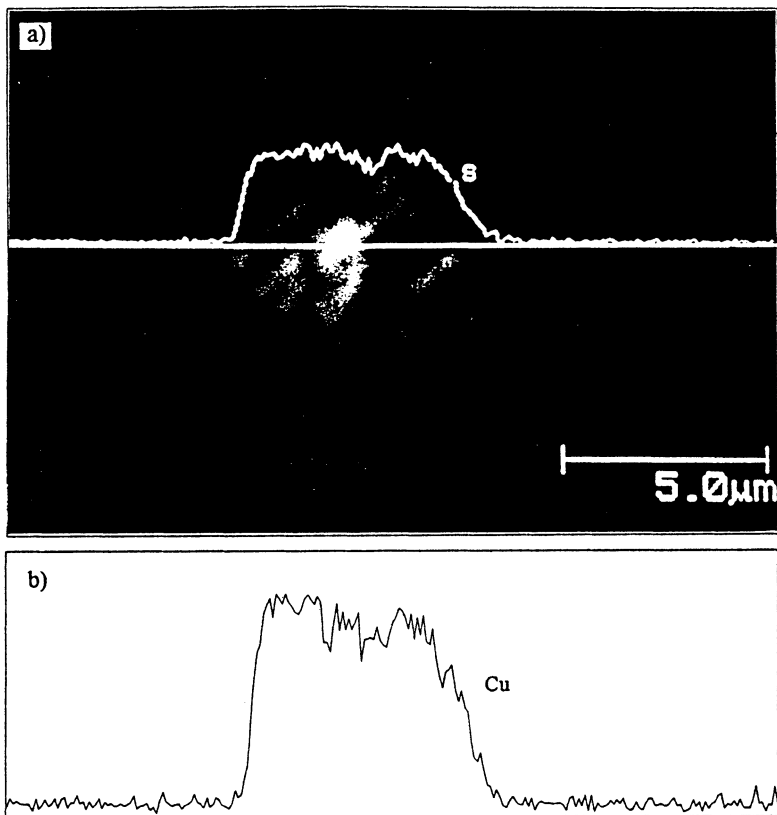


FIGURE 5: FE site containing Cu and S. (a) SEM image of the emitting site, (a,b) Auger line scan across the emitter (before sputtering) showing the S and Cu peak-to-peak height.

From our observation that non-emitting particles are sticking on the surface we believe that the heat treatment at 600°C–800°C activated the emission of particles that are already present on the cathode. This suggestion is strongly supported by segregation experiments in UHV performed with Auger spectrometer.^{23–26} It was found that the prevalent impurity on many transition metal surfaces like Nb, Mo, Ta, Ti or Au is sulfur. “Mild” heat treatments caused the sulfur to segregate at the surfaces of these materials. Almost all of the transition metals studied showed a very strong S peak (150 eV) after “short” heating to only 500°C. Heat treatments to 1000°C and higher normally removed the sulfur. On niobium the contaminants S, C, Cl, and O were found. Segregation experiments with Nb foils showed that heating at 300°C (even under ideal UHV conditions) promoted the segregation of O at the niobium surfaces even at 10 at.-ppm O impurity in the bulk.²⁷ Our results are also in accordance with the recent findings on reactor grade niobium¹⁰ where segregation phenomena stimulated the formation of MoS₂ which leads to enhanced field emission. From that point of view we suggest that impurities like O or S segregate at the niobium surface

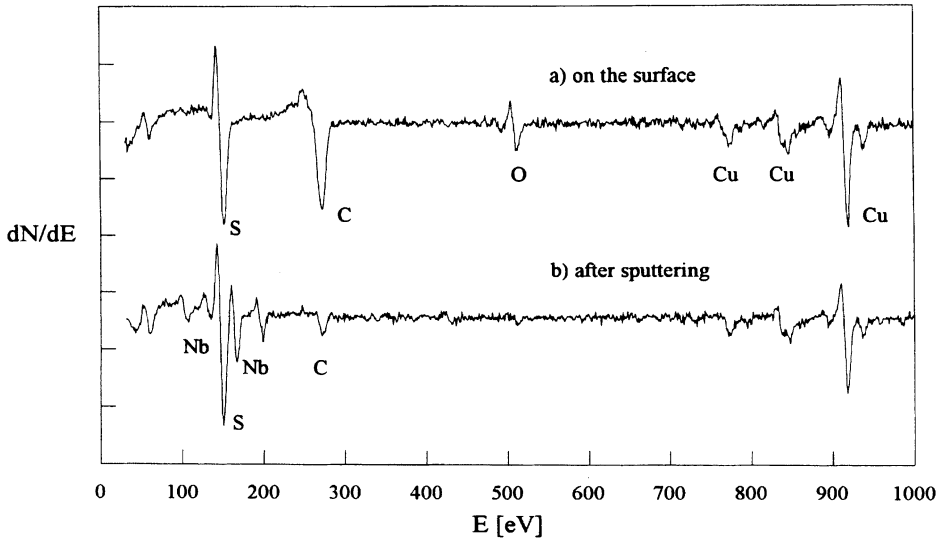


FIGURE 6: Point Auger spectra of the FE site of Figure 5, taken (a) on the surface and (b) after sputter removal of $\approx 300 \text{ \AA}$.

and form a MIM like contact in which the particle acts like an antenna probing the electrical field. In consequence, we believe that “very special” conditions are necessary at the interface between particle and cathode surface to promote the FE activity. In addition, the geometry of the particles may play an important role, because there could exist a geometric field enhancement that causes the emission. Our observation of the switch on of several sites at 200°C – 400°C cannot be explained with a simple protrusion model alone, because the sharp whisker will not be formed in this low temperature range.

8 STUDIES ON HIGH PRESSURE WATER RINSED CATHODES

One important and basic preparation technique of Nb cavities is the chemical polishing using BCP. With the hope to get a more defect free niobium surface a “damage layer” of ≈ 100 – $200 \mu\text{m}$ is normally removed. Little is known about the influence of surface damage removal on the field emission activity of DC cathodes and RF cavities. In this chapter we present results of 6 niobium samples that have been chemically polished between $4 \mu\text{m}$ and $84 \mu\text{m}$ using a 1:1:1 BCP. In addition a high pressure ultrapure water rinsing and a final methanol cleaning was performed. It should be pointed out that the cathodes were prepared at CEBAF (USA), shipped in our standard sample transport system, and tested in the field emission scanning microscope at Wuppertal. Full details of the preparation and characterization of the cathodes and the performed cavity measurements are published elsewhere.²⁸ In summary, no systematic dependence between emitter density and material removal up to $84 \mu\text{m}$ was observed in FE scans between 40 MV/m and 100 MV/m . SEM

images obtained at all localized sites in this study gave the very surprising result that the emission always originated at defects caused by surface irregularities like microscopic and macroscopic scratches. No emission sites were detected to be particles sticking on the surface. For the first time on a non heat treated broad area cathode 100 MV/m were reached on niobium without any electron field emission.²⁸ A selected area ($\approx 23 \mu\text{m BCP}$) was emission free even at 140 MV/m. These results are very promising for future investigations because a combination of surface smoothening (electropolishing) and high pressure rinsing with ultrapure water will probably result in an achievement of higher dc surface fields without prior high temperature heat treatments.

9 STATISTICS

In this chapter we present results obtained on nine different samples from high purity niobium. Three of them were prepared at Wuppertal using the standard 1:1:1 BCP followed by an ultrapure water rinsing. These samples were tested as introduced (no HT), during two thermal cycles between 1400°C and 200°C, and after high temperature treatments at 1400°C alone. The remaining six other samples were prepared at CEBAF as described in Chapter 8. The final cleaning step in the surface preparation of these cathodes was a high pressure ultrapure water rinsing followed by a rinsing with electronic grade methanol.²⁸ All these samples were scanned without the performance of any heat treatments. In Figure 7 the emitter density N/cm^2 versus

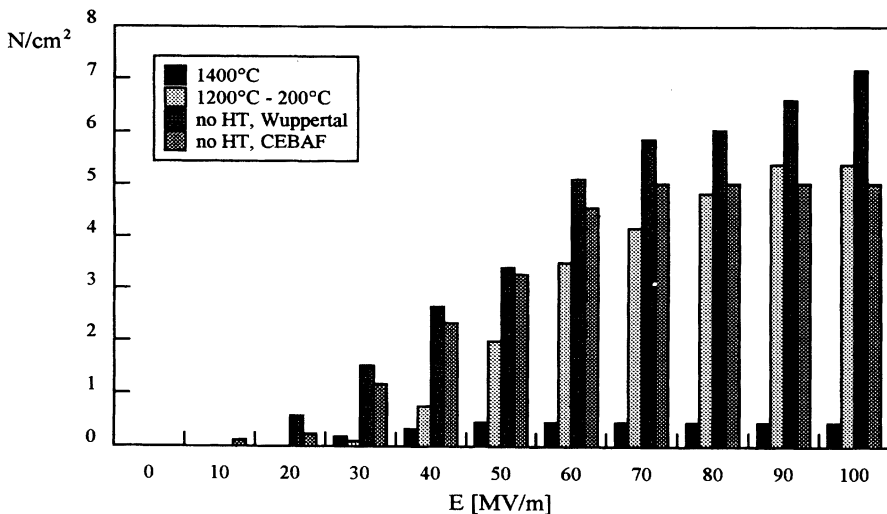


FIGURE 7: Histogram of the emitter density N/cm^2 as a function of the dc threshold field E measured at $I = 0.5$ nA.

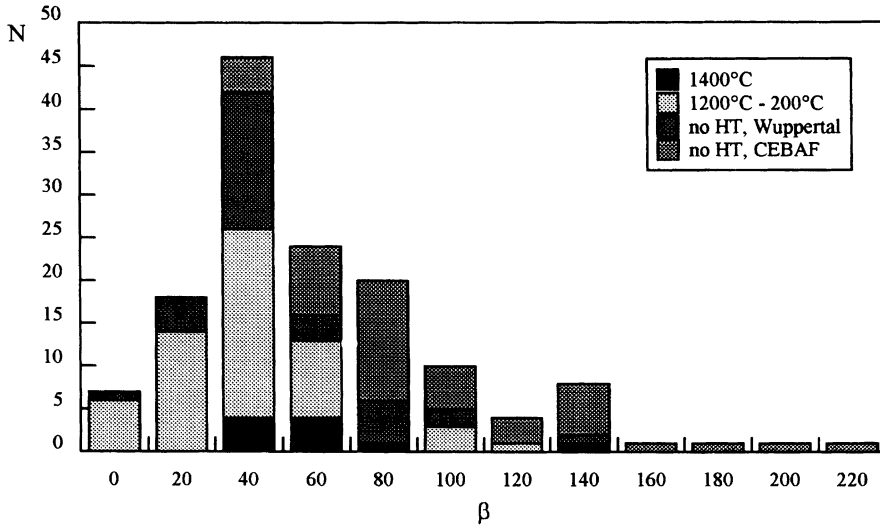


FIGURE 8: Histogram of the measured field enhancement factor β for all different sites analyzed in this dc study.

threshold field E is plotted. The best results were obtained after heating at 1400°C (30 min) resulting in ≈ 0.5 sites/ cm^2 between 50 MV/m and 100 MV/m. Non heat treated cathodes (no HT, Wuppertal & CEBAF) and heat treated samples at lower temperatures (200°C – 1200°C) showed a strong increase in emitter density with increasing surface field. Between 70 MV/m and 100 MV/m approximately 5 emitter/ cm^2 were detected on the CEBAF samples and the heated samples ($T < 1400^\circ\text{C}$) at Wuppertal. An increased density of sites ($\approx 7/\text{cm}^2$) was consistently found at a higher surface field (100 MV/m) on the as introduced Wuppertal samples.

The Fowler-Nordheim characteristics of all detected FE sites were individually measured during this study. A histogram of the field enhancement factor β of 141 different emitter is shown in Figure 8. On average, the detected “scratch emitter” (no HT, CEBAF) were identified as strong FE sites with “high” β values ranging between 49 and 239. Most of the other field emitter were identified as micrometer sized particles, their field enhancement factor β scattered between 7 and 150. In 91% of the scratches and surface irregularities the emitting areas S ranged between 10^{-10} and 10^{-16}cm^2 . The S values of the “standard” samples and especially cathodes after heat treatments (200°C – 1400°C) were found to be significantly larger and scattered between 10^{-8} and 10^{-16}cm^2 for 83% of the analyzed emitter. Even higher values than 10^{-8}cm^2 were measured in 17% of the analyzed sites. Because of the “nature” of field emitting sites found on the CEBAF samples²⁸ we believe that a preparation technique including a high pressure ultrapure water rinsing in a cleanroom might result in a lower density of sites at even higher surface fields in future applications.

10 CONCLUSION

We have characterized the field emission properties of high purity polycrystalline niobium samples as a function of heat treatment using our field emission scanning microscope. It was observed that a HT at 1400°C (30 min) normally switched off all FE sites and an “electrically clean” ($I < 10$ nA) surface was consistently obtained at 100 MV/m. After heating such a sample at 600°C–800°C a strong increase in the density of field emitting sites was reproducibly detected on high purity (RRR = 270) bulk niobium. It is remarkable that annealing a sample for only 30 min at low temperatures of 200°C and 400°C activated 13 additional emitter. In SEM studies of all localized sites isolated particles with random shapes were found. Point Auger spectra on that kind of field emitter showed that the analyzed particles contained Al, W, Ca, Ti, Cu, S, C, O, and Nb. From our observation that non-emitting particles are sticking on the surface we believe that the heat treatments at “low” temperatures can activate the emission of particles which are already present on the cathode surface. We suggest that impurity segregation at the niobium surface either activates or creates field emitting sites even on high purity niobium samples. No influence of adsorbed O_2 on the density of sites and their spatial distribution was found during a test series of gas exposure experiments.

In Saclay various kinds of particles with known shape and composition were intentionally placed on Nb and Au cathodes. Irregular-shaped particles were associated with “good” emitter while most of the spherical particles did not emit up to 120 MV/m. No relation between particle size (3–20 μm) and field emission threshold was found for irregular FE sites. In summary, the Saclay experiments seem to indicate that the interface between intentionally positioned particles and the substrate (Nb and Au) does not play an important role. A “projection on a projection” model has been proposed that might explain the observed geometry and the measured β of the studied artificial sites.

In several experiments on 6 different samples of the same high purity sheet niobium the dependence of the electron field emission behaviour on incremental material removal was studied at Wuppertal and CEBAF. For these investigations the final cleaning step in the surface preparation was a high pressure ultrapure water rinsing followed by a rinsing with electronic grade methanol. No systematic dependence between emitter density and material removal between 4 μm and 84 μm was observed in FE scans up to 100 MV/m. For the first time no sites were detected at 100 MV/m on a non heat treated broad area niobium cathode. In contrast to earlier investigations the electron emission always originated from material irregularities without the presence of microscopic particles sticking on the surface. Therefore, no “intrinsic” field emitter were found if surface imperfections are not counted in this category. These results are very promising for future high voltage applications because a combination of surface smoothing and high pressure ultrapure water rinsing might result in a further reduction of electron emission at even higher surface fields.

ACKNOWLEDGEMENTS

I am very grateful to N. Pupeter for his enthusiastic support, H. Piel and G. Müller for many fruitful discussions during our experiments. It is a pleasure to thank P. Kneisel for excellent sample preparation, D. Proch and H. Peters for their support during the Auger experiments.

The author wishes to thank R.V. Latham, N.S. Xu, Ø. Fischer, M. Jimenez, and B. Bonin for kindly providing the latest information on their laboratory activities. This work was funded in part by the German Federal Minister for Research and Technology under the contract number 055WT8517.

REFERENCES

1. R.V. Latham, *High Voltage Vacuum Insulation: The Physical Basis* (Academic Press, London 1981).
2. D. Alpert, D.A. Lee, E.M. Lyman, H.E. Tomaschke, *J. Vac. Sci. Technol.*, **1** (1964) 35.
3. R.J. Noer, *Appl. Phys.*, **A28** (1982) 1.
4. B.M. Cox, *J. Phys. D: Appl. Phys.*, **8** (1975) 2065.
5. R.E. Hurley, *J. Phys D: Appl. Phys.*, **12** (1979) 2247.
6. C.S. Athwal, R.V. Latham, *Physica*, **104C** (1981) 46.
7. Ph. Niedermann, N. Sankarraman, Ø. Fischer, *Proc. of the 2nd Workshop on RF Superconductivity*, (Geneva 1984), p. 583.
8. E. Mahner, N. Minatti, H. Piel, N. Pupeter, *Appl. Surf. Science*, **67** (1993) 23.
9. B.M. Cox, in *Proceedings of the VI Int. Symp. on Discharges and Electric. Insul.*, (Swansea 1974) p. 135.
10. Ph. Niedermann, PhD thesis No. 2197, University of Geneva, 1986.
11. N.K. Allen, R.V. Latham, *J. Phys. D: Appl. Phys.*, **11** (1978) L55.
12. R.V. Latham, *IEEE Trans. on Electric. Insul.*, **23** (1988) 9.
13. K.H. Bayliss, R.V. Latham, *Proc. R. Soc. London*, **A403** (1986) 285.
14. C.S. Athwal, R.V. Latham, *J. Phys. D: Appl. Phys.*, **17** (1984) 1029.
15. N.S. Xu, R.V. Latham, *Surf. Science*, **274** (1992) 147.
16. N.S. Xu, R.V. Latham, *Vacuum*, **43** (1992) 99.
17. M. Jimenez, R.J. Noer, G. Jouve, C. Antoine, B. Bonin, *J. Phys. D: Appl. Phys.*, **26** (1993) 1503.
18. D. Bloess, in *Proceedings of the 2nd Workshop on RF Superconductivity* (Geneva, 1984) p. 409.
19. J.M. Jimenez, R.J. Noer, G. Jouve, J. Jodet, B. Bonin, submitted to *J. Phys. D: Appl. Phys.*, 1993.
20. A.D. Archer, R.V. Latham, *XIVth Int. Symp. on Discharges and Electric. Insul.*, Santa Fe, 1990.
21. Ph. Niedermann, N. Sankarraman, R.J. Noer, Ø. Fischer, *J. Appl. Phys.*, **59** (1986) 892.
22. The measurements were done by J. Scholtes, IFOS, Kaiserslautern, Germany.
23. T.W. Haas, J.T. Grant, G.J. Dooley, *J. Vac. Sci. Technol.*, **7** (1969) 43.
24. L.A. Harris, *J. Appl. Phys.*, **39** (1968) 1428.
25. S. Hofmann, *Vacuum*, **40** (1990) 9.
26. S. Hofmann, *Materials Science Engineering*, **42** (1980) 55.
27. S. Hofmann, G. Blank, H. Schultz, *Z. Metallkde.*, **67** (1976) 189.
28. E. Mahner, P. Kneisel, N. Pupeter, G. Müller, in *Proceedings of the 6th Workshop on RF Superconductivity* (Newport News, 1993), to be published.